Nuclear Resonant Magnetometry and its Application to Fe/Cr Multilayers

C. L'abbé* and J. Meersschaut

Instituut voor Kern-en Stralingsfysica, Katholieke Universiteit Leuven, Celestijnenlaan 200D, B-3001 Leuven, Belgium
Argonne National Laboratory, 9700 South Cass Avenue, Argonne, Illinois 60439, USA

W. Sturhahn, J. S. Jiang, T. S. Toellner, E. E. Alp, and S. D. Bader

Argonne National Laboratory, 9700 South Cass Avenue, Argonne, Illinois 60439, USA

(Received 25 February 2004; published 12 July 2004)

We introduce nuclear resonant magnetometry as a means to record the magnetization curve of isotopically enhanced regions of a sample. It is based on nuclear resonant scattering with circularly polarized synchrotron radiation and the use of a nuclear resonant reference sample. We apply this approach to study the interlayer coupling in Fe/Cr(100) multilayers and to obtain a layer-specific magnetization curve. Our measurements provide experimental evidence for the existence of a nontrivial interlayer-coupling angle in Fe/Cr/Fe.

DOI: 10.1103/PhysRevLett.93.037201 PACS numbers: 75.60.Ej, 75.25.+z, 75.70.–i, 76.80.+y

In this Letter, we present the application of a new experimental technique that selectively probes the magnetization of well-defined parts of the sample. The technique is based on nuclear resonant scattering of synchrotron radiation [1], and relies on the isotope selectivity of the scattering process. By replacing certain regions of the sample with the resonant isotope, one can measure these specific sites selectively [2]. Nuclear resonant scattering of synchrotron radiation permits one to study magnetization properties via the hyperfine interactions acting on the resonant nuclei [3–6]. However, since synchrotron radiation is usually linearly polarized, the sign of the magnetization vector cannot be retrieved, thus limiting the accessible information. The innovative part of this work is that we performed nuclear resonant scattering with *circularly* polarized x rays and were able also to measure the sign of the magnetization vector. In the following, we explain this approach and show an experimental application where we study the interlayer coupling in Fe/Cr(100) multilayers.

The interlayer coupling in Fe/Cr was first discovered in 1986 [7]. Depending on the Cr thickness, the magnetization in subsequent Fe layers will order parallel or antiparallel, or perpendicular to each other. Apart from this well-established bilinear and biquadratic coupling, also the existence of noncollinear interlayer coupling has been reported, where the coupling angle deviates from 0°, 90°, or 180° [8]. The results of Ref. [8] were obtained by means of polarized neutron reflectometry on Fe/Cr multilayers. Recently, however, attention was drawn to the fact that surface effects, due to the reduced symmetry at the boundary of the multilayer stack, can have a considerable influence on the results [9,10]. In the present investigation, we exclude surface effects and explore the existence of noncollinear ordering in Fe/Cr(100).

We prepared a Fe(50 Å)/Cr(11 Å)/Fe(50 Å)/Cr(11 Å)/Fe(50 Å) quintalayer consisting of three Fe layers of equal thickness. For Cr thicknesses of 11 Å, one expects strong antiferromagnetic interlayer coupling. When a large external field is applied along an easy axis, the magnetization in all three Fe layers will be oriented along the external field. With decreasing field, however, the Zeeman interaction will keep the outer Fe layers along the field, while the antiferromagnetic interlayer coupling will gradually pull the inner Fe layer in the opposite direction. If the interlayer coupling is purely antiferromagnetic, one expects the angle between the inner and the outer magnetization vectors to be 180° near zero field. Since the interlayer coupling mainly affects the inner magnetization vector, one can study the coupling directly by selectively measuring the orientation of the magnetization in the central Fe layer. Therefore, the central layer is fabricated from the nuclear resonant ^{57}Fe isotope, while the two outer layers consist of nonresonant ^{56}Fe. This isotopic distinction between the inner and the outer Fe layers has no influence on the electronic and magnetic properties of the multilayer, yet it enables one to measure the magnetization of the central layer selectively with nuclear resonant scattering of synchrotron radiation.

The resonant nuclei, in our case ^{57}Fe, are excited by a synchrotron pulse through absorption of a 14.413 keV photon. When the nuclei deexcite through the coherent elastic channel, a photon with the same energy is emitted. The resonantly scattered photons are detected as a function of the time that has elapsed after the arrival of the incident synchrotron pulse. Apart from a decaying intensity related to the lifetime of the excited state (141 ns in the case of ^{57}Fe), the time spectra show rapid oscillations. These are quantum beats originating from the hyperfine splitting of the nuclear states [11]. In the case of a magnetic interaction, the hyperfine splitting is proportional to the total magnetic field $\vec{B}_{\mathrm{tot}}$ at the position of the nucleus, i.e., the sum of the internal hyperfine field $\vec{B}_{\mathrm{hf}}$ and the externally applied field $\vec{B}_{\mathrm{ext}} = \mu_0 \vec{H}$. From early Mössbauer experiments, it is known that the orientation of the internal hyperfine field is strongly correlated to that

of the magnetization vector $\vec{M}$ [12]. For example, for iron the ^{57}Fe hyperfine field is oriented antiparallel to the magnetization vector [13], and has a value of -33.0 T at room temperature [14]. Analysis of the quantum beats permits an accurate determination of the hyperfine field, and thus also of the magnetization vector.

With linearly polarized synchrotron radiation, one cannot distinguish between two antiparallel directions of the hyperfine field; hence, the sign of the magnetization vector cannot be retrieved [15]. Sign sensitivity can be obtained when the incoming photons are circularly polarized. A photon with left circular polarization has helicity $+1$ [16]. As a consequence, it can couple only to nuclear transitions which require an angular momentum change $\Delta m = +1$, provided the quantization axis for the hyperfine interaction is parallel to the photon direction ($\vec{B}_{\rm tot} || \vec{k}$), or $\Delta m = -1$ transitions if the quantization axis is antiparallel to the photon direction ($\vec{B}_{\rm tot} || -\vec{k}$). The insets of Figs. 1(a) and 1(b) show that switching the sign of the hyperfine interaction will select different nuclear resonances. When the quantization axis for the hyperfine interaction is not aligned with the photon direction $\vec{k}$, then the photon eigenstates get mixed when expressed in the principal axis system of the hyperfine interaction. As a result, the $\Delta m = +1$ and -1 transitions are excited simultaneously, as well as the $\Delta m = 0$ transitions. As long as the hyperfine field, and therefore the magnetization vector, has a nonzero component along $\vec{k}$, the strength of the $\Delta m = +1$ and -1 transitions will be different, so that the nuclear resonant scattering remains sensitive to the sign of the hyperfine field.

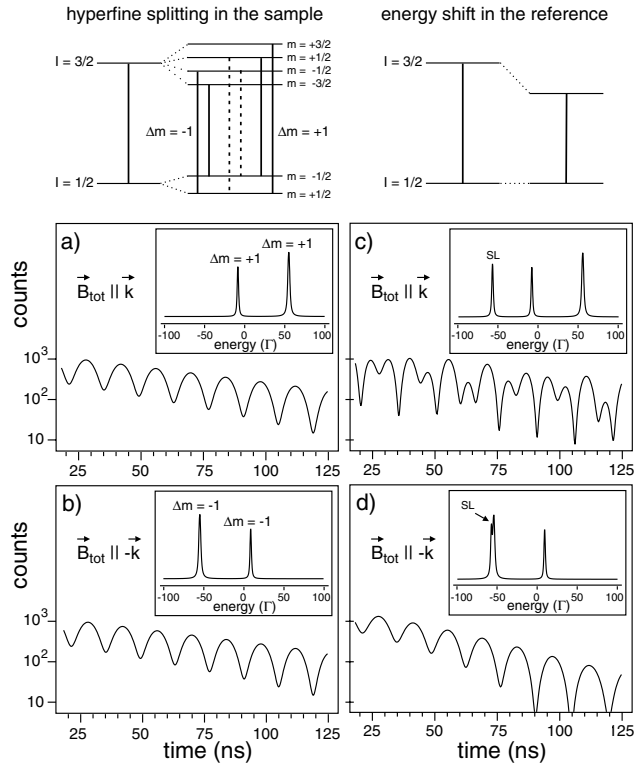

FIG. 1. Simulations for nuclear resonant forward scattering with left circularly polarized radiation. (a),(b) Simulations for a 0.5 μm ^{57}Fe foil with a hyperfine field of -33 T either parallel or antiparallel to the photon direction $\vec{k}$. (c),(d) Simulations with an additional 0.15 μm single-line reference sample (SL) whose nuclear transition is shifted by -58Γ ($\Gamma = 4.65$ neV). The insets show the nuclear resonance lines in the energy domain relative to 14.413 keV. Schematic energy level schemes for the sample and the reference are shown on top.

As nuclear resonant scattering experiments with synchrotron radiation are performed in the time domain, one does not observe the nuclear transitions directly, but instead one observes the quantum beating between different transitions. This quantum beating depends only on the strength of the nuclear transitions and their energy separation. For a magnetic interaction, the relative strengths of the transitions as well as the energy separations remain identical when the sign of the hyperfine field is inverted. Consequently, the time spectra are exactly the same for both orientations [see Figs. 1(a) and 1(b)]. To break this inversion symmetry in the time domain, a single-line reference sample was added whose nuclear transition energy is shifted with respect to the central transition energy in the sample under investigation. As a result, the energy separations between different lines are no longer the same for opposite field directions and the corresponding time spectra are clearly distinct. This is illustrated in Figs. 1(c) and 1(d). The introduction of circularly polarized x rays in nuclear resonant scattering and the use of a nuclear resonant reference sample to break the inversion symmetry in the time domain now permits one to extract the full magnetization information including the sign. This approach, which we will refer to as nuclear resonant magnetometry (NRM), is applied to investigate the interlayer coupling in the Fe/Cr(100) quintalayer.

The sample was grown by dc magnetron sputtering onto a MgO(100) substrate as described in Ref. [17]. A 111 Å Cr buffer was first deposited at 400 °C to improve the epitaxial growth. The ^{56}Fe(50 Å)/Cr(11 Å)/^{57}Fe(50 Å)/Cr(11 Å)/^{56}Fe(50 Å) quintalayer was subsequently grown at 110 °C. Finally, the whole structure was capped with 44 Å Cr to prevent oxidation. The sample composition and quality were verified with Cu-Kα x-ray diffraction both at low and high angles. The magnetization of the sample as a whole was measured with an alternating gradient magnetometer. The result [shown in Fig. 4(b)] provides the magnetic response of all three Fe layers. The magnetization of only the central Fe layer was measured with NRM.

The NRM measurements were performed at the 3ID beam line of the Advanced Photon Source [18]. The storage ring produced single x-ray pulses every 153 ns. The radiation was monochromatized to 1.3 meV around the 14.413 keV nuclear resonance of ^{57}Fe. Figure 2 shows the experimental setup after the high-resolution monochromator. For measurements with circularly polarized

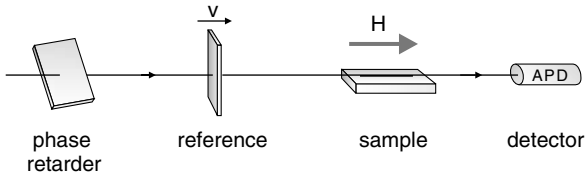

FIG. 2. Setup for nuclear resonant magnetometry.

radiation, a Bragg transmission phase retarder was used to convert the polarization state of the x rays from linear to circular [19]. It consists of a 400 μm C(111) single crystal with its diffracting planes inclined at 45° with respect to the synchrotron plane. The offset angle of the phase retarder from the exact Bragg condition was -0.080 mrad, corresponding to a theoretical value for left circular polarization of 87%. A 1-μm stainless steel foil (SS310, enriched in ^{57}Fe) was used as the single-line reference sample. It was mounted on a constant velocity drive set to -5.6 mm/s, so that the resonance is shifted by -58Γ. Finally, the Fe/Cr quintalayer sample was placed at a grazing angle of 3.6 mrad. An external magnetic field was applied along the incident photon direction $\vec{k}$ and parallel to the in-plane easy axis of the sample. The nuclear resonant scattering intensity was recorded as a function of time by means of an avalanche photodiode detector.

Figure 3 shows selected spectra for different external field values taken with linearly polarized radiation (without the phase retarder or reference sample) and with circularly polarized radiation (using the phase retarder and reference sample). The spectra were analyzed using the CONUSS fitting routine [20], based on the dynamical theory of nuclear resonant scattering [21]. The spectra in Fig. 3 are very sensitive to the magnitude and the orientation of the magnetization vector in the central Fe layer. However, the linear spectra only allow one to determine the magnetization vector up to a parity transformation; i.e., the projection of the magnetization vector on the photon direction can either be positive or negative. From the fits of the circular spectra, also the sign of the magnetization vector can be extracted. The latter is illustrated by comparing the linear and circular spectra taken at -7 mT and $+25$ mT. The linear spectra show almost no difference, both yield angles between $\vec{M}$ and $\vec{k}$ close to 40° or 140°. The circular spectra, on the other hand, are quite distinct from each other. The spectrum at -7 mT shows a slow oscillation, indicating that the projection of the magnetization vector on the photon direction $\vec{M} \cdot \vec{k}$ is positive, and, hence, the angle is 40(3)°. The spectrum at $+25$ mT shows a much faster oscillation, indicating that $\vec{M} \cdot \vec{k}$ is negative, and, hence, the angle is 135(2)°.

All spectra were fitted with two hyperfine field contributions. The main contribution (88%) reflects the magnetization in the core of the ^{57}Fe layer. The other contribution (12%) accounts for the interface regions (3 Å at each interface). For the core, we found a magnetic

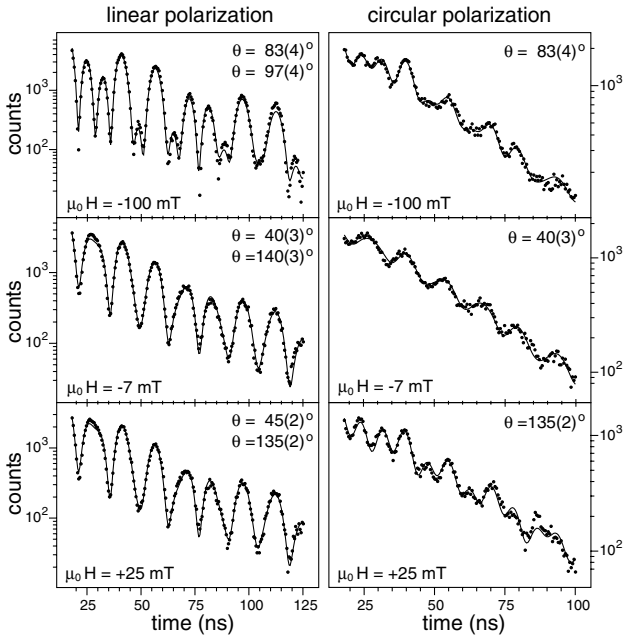

FIG. 3. Experimental time spectra for different external field values taken with linearly polarized radiation (left) and circularly polarized radiation (right). The line represents the theoretical fit to the data. θ is the in-plane angle between $\vec{M}$ and $\vec{k}$ obtained from the fit.

hyperfine field $B_{\mathrm{hf}} = -33.0(3)$ T. A small Lorentzian distribution with FWHM = 0.08(1) T was included. The interface showed a reduced hyperfine field $B_{\mathrm{hf}} = -31.7(5)$ T [22] with a distribution FWHM = 0.07(5) T.

For each external field value, we were thus able to determine the magnetization vector in the ^{57}Fe layer. Plotting the projection of the magnetization on the external field direction as a function of the field strength yields a nuclear resonant magnetization curve as shown in Fig. 4(a). It is important to note that this is an isotope-selective magnetization curve reflecting the magnetic response of the central Fe layer only. This independent information adds to the macroscopic magnetization curve shown in Fig. 4(b) which reflects the response of all Fe layers simultaneously. Combining both curves and assuming the two outer Fe layers are identical, one can determine the magnetization direction in each Fe layer separately. Let φ be the angle between the outer magnetization vectors and the external field and θ be the angle between the central magnetization vector and the external field. The macroscopic magnetization [Fig. 4(b)] is then given by $(2\cos\varphi + \cos\theta)/3$. Since $\cos\theta$ is known from the NRM results [Fig. 4(a)] the angle φ can be calculated. Finally, also the angle between the central and the outer magnetization vectors, $|\theta - \varphi|$, can be determined. The latter is displayed in Fig. 4(c), and contains direct and detailed information on the interlayer coupling. For example, at remanence we find an angle between subsequent Fe layers of 162(4)°, which confirms the existence of noncollinear interlayer coupling in the Fe/Cr(100)

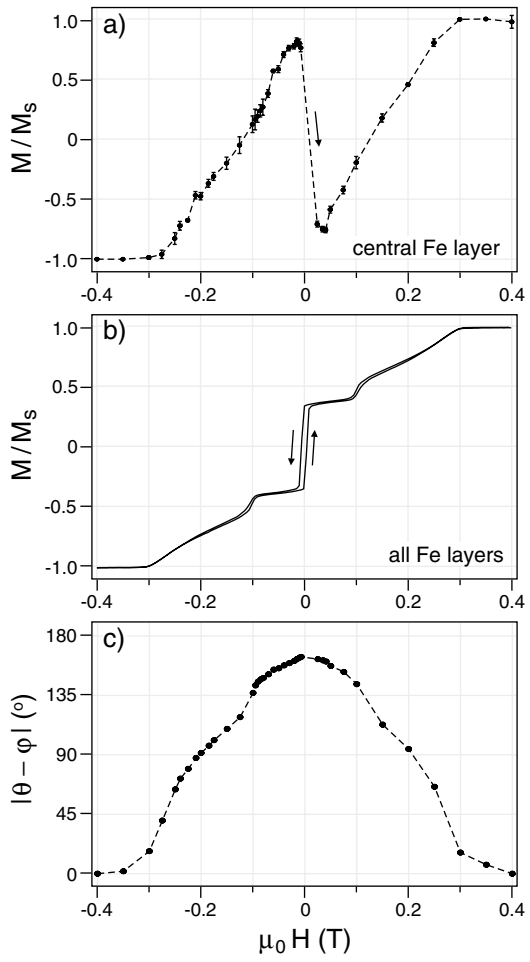

FIG. 4. Magnetization measurements with the applied field along one of the easy axes in the sample. (a) Magnetization curve obtained via nuclear resonant magnetometry. (b) Macroscopic magnetization curve. (c) Angle between the magnetization vectors in the central and the outer Fe layers obtained from the curves (a) and (b) as explained in the text.

multilayer. Indeed, the fact that the angle at remanence deviates from 180° proves that the interlayer coupling is not purely antiferromagnetic, but contains noncollinear contributions.

In conclusion, by introducing circularly polarized radiation in nuclear resonant scattering we were able to measure an isotope-selective magnetization curve. The sign sensitivity, which is crucial for a correct interpretation of the results, was obtained by including a nuclear resonant reference sample mounted on a constant velocity drive. It was shown how nuclear resonant magnetometry can be used for layer-selective magnetization measurements in multilayers and thin films. Thanks to the high brilliance of third-generation synchrotrons, nuclear resonant magnetometry can in the future be applied to even smaller structures with submonolayer coverage of the resonant isotope. We therefore believe that the technique can have a wide range of applications in magnetism research.

It is a pleasure to thank R. Callens for fruitful discussions. The authors are also grateful to D. Brown, J. Burke, C. Kimball, J. Pearson, and J. Zhao for their support. Work at Argonne was funded by the U.S. DOE Office of Science under Contract No. W-31-109-Eng-38. Work at Leuven was supported by the Fund for Scientific Research Flanders and the Inter-University Attraction Pole (IUAP P5/1). C. L'abbé and J. Meersschaut thank the Belgian Science Foundation (F.W.O.-Vlaanderen).

*Electronic address: caroline.labbe@fys.kuleuven.ac.be

[1] Special issues on *Nuclear Resonant Scattering of Synchrotron Radiation* [Hyperfine Interact. **123/124** (1999); **125** (2000)].
[2] T. Shinjo and W. Keune, J. Magn. Magn. Mater. **200**, 598 (1999).
[3] L. Niesen *et al.*, Phys. Rev. B **58**, 8590 (1998).
[4] R. Röhlsberger *et al.*, Phys. Rev. Lett. **89**, 237201 (2002).
[5] R. Röhlsberger *et al.*, Phys. Rev. B **67**, 245412 (2003).
[6] D. L. Nagy *et al.*, Phys. Rev. Lett. **88**, 157202 (2002).
[7] P. Grünberg *et al.*, Phys. Rev. Lett. **57**, 2442 (1986).
[8] A. Schreyer *et al.*, Europhys. Lett. **32**, 595 (1995).
[9] V. Lauter-Pasyuk *et al.*, Phys. Rev. Lett. **89**, 167203 (2002).
[10] S. G. E. te Velthuis *et al.*, Phys. Rev. Lett. **89**, 127203 (2002).
[11] E. Gerdau *et al.*, Phys. Rev. Lett. **57**, 1141 (1986).
[12] G. J. Perlow *et al.*, Phys. Rev. Lett. **4**, 74 (1960).
[13] S. S. Hanna *et al.*, Phys. Rev. Lett. **4**, 513 (1960).
[14] U. Bergmann *et al.*, Phys. Rev. B **50**, 5957 (1994).
[15] One could determine the sign of the hyperfine field by observing whether the hyperfine splitting increases or decreases on application of a large external field. This approach, however, cannot be used for magnetization measurements since the sign information should also be accessible in the presence of small external fields where the sample is not necessarily in saturation.
[16] We follow the convention of J. D. Jackson, *Classical Electrodynamics* (Wiley, New York, 1975).
[17] E. E. Fullerton *et al.*, Phys. Rev. B **48**, 15 755 (1993).
[18] http://www.aps.anl.gov
[19] K. Hirano, T. Ishikawa, and S. Kikuta, Nucl. Instrum. Methods Phys. Res., Sect. A **336**, 343 (1993).
[20] W. Sturhahn, Hyperfine Interact. **125**, 149 (2000).
[21] J. P. Hannon and G. T. Trammell, Phys. Rev. **169**, 315 (1968); **186**, 306 (1969).
[22] In Refs. [23,24], the interface region is modeled by six reduced hyperfine field components. However, due to the predominant contribution of the core region in our spectra, we are not sensitive enough to the interface to allow for such a detailed hyperfine field modeling. We opted to use only one interface component since this gave already exceptionally good fit results.
[23] T. S. Toellner *et al.*, Phys. Rev. Lett. **74**, 3475 (1995).
[24] V. M. Uzdin *et al.*, Phys. Rev. B **63**, 104407 (2001).